Twisting & Bending Performance of a Subscale CORC® Cable-in-Conduit-Conductor for Fusion and Detector Magnet Applications

Michael Naus, Hugh Higley, Maxwell Maruszewski, Soren Prestemon, *Senior Member, IEEE*, Kyle Radcliff, Danko van der Laan, *Senior Member, IEEE*, Xiaorong Wang, and Jeremy Weiss, *Member, IEEE*

***Abstract*—Future magnetic confinement fusion machines and detector magnets will likely utilize high temperature superconducting (HTS) wire and/or tapes, configured in a Cable-in-Conduit-Conductor (CICC) to generate magnetic fields at temperatures above 4.2 K. As such, these CICCs will need to be twisted & bent to meet the design criteria for any given machine. We investigated the critical current (I_c) degradation of a subscale 6-around-1 CICC using Conductor-on-Round-Core® (CORC®) wires after ever increasing deformation. A CORC® wire was inserted into one of six outer openings of an extruded aluminum conduit to form a sub-scale CICC, after which the CICC was twisted to ∼25 cm pitch and the whole assembly was then sequentially bent to nominal radii of ∼50 cm, ∼35 cm, and ∼25 cm. The I_c values at 77 K and self-field when straight and after each deformation step was measured. The CORC® wire I_c was robust to this type of "twisting + bending" deformation, with an overall degradation of ∼10% with respect to the straight, non-twisted wire. We also describe a CICC twisting process that potentially allows twisting of continuous-length CICCs after the CORC® wires are inserted. This method can lead to a scalable fabrication process of long-length CORC® CICCs that are required for manufacture of high-field fusion magnets and detector magnets for high-energy physics research.**

***Index Terms*—CORC®, critical current, deformation, detector, fusion, high temperature superconductor, HTS, ReBCO.**

I. Introduction

FUTURE magnetic confinement fusion machines and accelerator detector magnets might use high temperature superconductors (HTS), due to their better high magnetic field and high temperature performance than that of low temperature superconductors (LTS) [1], [2], [3]. Also, Cable-in-Conduit-Conductor (CICC) designs offer advantages in the manufacture of such large machines. CICCs help to define a conductor 'unit' of known dimension, independent of the superconductor used inside. They also offer some benefit where redistribution between strands is significant [4], (i.e., where critical current differences between strands, wires, or tapes is significant). This is the case with Rare-earth Barium Copper Oxide (ReBCO) tapes. While ReBCO tapes appear to be not ideal for CICC designs due to their highly aspected geometry [4], multi-tape wires can ameliorate this limitation.

Any CICC will need to be twisted and bent to varying degrees, depending on a machine's given design. The two-dimensional (2D) bending performance of individual ReBCO tapes and of multi-tape cables, as well as those helically wound around a central tube or grooved former, has been reported [5], [6], [7], [8], [9], [10], [11], [12], [13]. However, each multi-tape conductor and each conductor-in-CICC assembly is unique, and the in-situ twisting + bending performance of CORC®-in-CICC has not yet been reported. Here, we report on the I_c performance of a sub-scale 6-around-1 Al CICC design utilizing ReBCO CORC® wires after twisting and bending deformation.

II. Methodology

A. CORC® Samples

CORC® wire samples were manufactured and provided by Advanced Conductor Technologies (ACT). All wires were 3.7 mm in diameter with 30 ReBCO tapes helically wound around a 2.5 mm Cu wire in 12 layers. The tapes were 2 mm wide with 30 µm substrates. The tapes for Wires #1 and #2 were from SuperPower, Inc., and Wire #3 used tapes from Shanghai Superconductor Technology Co (SST). Wires #1 and #2 were cut from the same source spool of CORC® wire. All wires have 30 µm thick polyester heat shrink tubing as electrical insulation. The vendor-provided I_c values of the SuperPower and SST tapes at 77 K in self-field were 56 A and 84 A, respectively.

B. CORC® Terminations

The CORC® wires were terminated in a similar fashion to those described in [14], which is slightly different than the ACT

Received 25 September 2024; revised 13 November 2024 and 5 December 2024; accepted 6 December 2024. Date of publication 30 December 2024; date of current version 22 January 2025. This work was supported in part by the U.S. Department of Energy, Office of Fusion Energy Sciences under Contract DE-AC02-05CH11231 and Contract DE-SC0018125, and in part by the Office of High Energy Physics under Contract DE-SC140009. *(Corresponding author: Michael Naus.)*

Michael Naus, Hugh Higley, Maxwell Maruszewski, Soren Prestemon, and Xiaorong Wang are with Lawrence Berkeley National Laboratory, Berkeley, CA 97240 USA (e-mail: naus@lbl.gov).

Kyle Radcliff is with Advanced Conductor Technologies, Boulder, CO 80301 USA (e-mail: kyle@advancedconductor.com).

Danko van der Laan and Jeremy Weiss are with Advanced Conductor Technologies, Boulder, CO 80301 USA, and also with the University of Colorado, Boulder, CO 80309 USA (e-mail: danko@advancedconductor.com).

Color versions of one or more figures in this article are available at https://doi.org/10.1109/TASC.2024.3520068.

Digital Object Identifier 10.1109/TASC.2024.3520068

patented method but still falls within said patents [15], [16]. For this application, commercially available oxygen-free high-conductivity (OFHC) Cu tubes with Ø7.94 mm (0.3125 inch) outer diameter (OD) were used. The 20 cm long Cu tubes had a straight line of Ø3.2 mm (0.125 inch) holes drilled every 5.1 mm (0.2 inch). Voltage taps were placed on the Cu core, at the center of the termination tube, and at inner end of the termination tube, nearest to the to-be-twisted conduit.

Once all tapes were cut and inside the Cu tube, pieces of Al foil were used as tube endcaps to contain the subsequent liquid indium. The tube was heated to ∼170 °C Alpha 260-HF flux (from MacDermid Alpha) was squirted into the line of holes with a syringe when temperatures exceeded ∼120 °C. This was followed by indium shavings being laid onto the holes. As the indium melted, it drained through the holes and into the Cu tube. Once the tube was full (as evidenced by lack of bubbles coming through the liquid indium), heating was stopped and compressed air blown through the heating assembly to hasten cool down.

Since the holes in the conduit were smaller than the Cu tube (i.e., termination) diameter, one CORC® wire end was terminated as described, then the CORC® wire was inserted into the conduit, and then the other end was terminated.

Approximately 10 cm of "free" CORC® wire was left between the end of the conduit and the termination to help accommodate any inadvertent stresses on the CORC® wire.

C. Cu Clamps

For testing, the Cu tube terminations were clamped between two pieces of machined Cu. Each is approximately 9 mm thick and 33 mm wide. The lengths of the Cu clamp halves were different at 200 mm and 250 mm, with the extra 50 mm for power supply cable attachment. Both halves have a semi-circular groove for the Cu tube termination to fit in.

Between all surfaces (clamp-to-termination and clamp-to-clamp), a ∼125 μm layer of indium was applied to ensure good electrical connectivity. The clamps were then uniformly tightened with 16 #10–32 bolts (8 per side) to ∼340 N·cm (30 in·lbs) each.

Once clamped, each assembly of conduit, CORC®, termination, and clamp was secured together using a G-10 plate (shown later). This eliminated the risk of inadvertent strain on the exposed CORC® wire between the conduit and termination.

D. The Conduit & Twisting

The Al conduit (Fig. 1), provided by ACT and with a design first discussed in [17], was designed with nominal dimensions in order to be able to be used with CORC® wires of various diameters. It had a 20 mm diameter, with six Ø5 mm outer openings around a central Ø6.3 mm opening. There are small grooves on the conduit exterior equidistant between the outer Ø5 mm openings. These were used to help the purpose-built collet hold the conduit during twisting, through the use of Cu pins, seen in Fig. 1(c).

Once the CORC® wire was in the ∼1.25 m long conduit, terminated on both ends, and Cu clamps attached, it was I_c tested while straight. The conduit was then twisted at room temperature

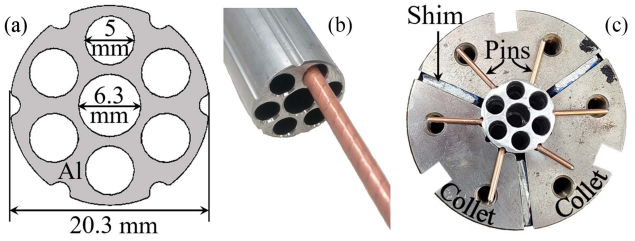

Fig. 1. (a) Al conduit cross-sectional drawing. (b) Conduit with CORC® wire in one outer opening. (c) Conduit in 3-part collet with shims between collet pieces and folded-over restraining pins.

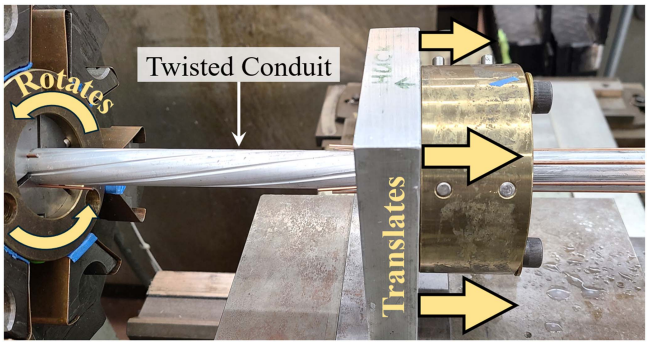

Fig. 2. A new conduit twisting technique. A non-rotating collet translates down-length in synchronicity with a non-translating rotating collet.

by one of two methods, which would put the CORC® wire into a helical shape within.

In the first method, Wires #1 & #2 were twisted simply by securing each end in a collet, with one of those collets in the jaws of a lathe. That lathe was manually turned using a lever arm, and the entire conduit length was twisted to the target twist pitch of ∼25 cm.

The 2nd twisting method used a novel approach and was used on Wire #3 (Fig. 2). It again had one end in a collet in a lathe for manual turning. The other collet, however, was set as close to the lathe as possible. This 2nd collet had shims between the collet pieces, so that it was just loose enough to translate down length, but still be tight enough so that the pins engaged with the exterior conduit grooves and the matching grooves in the collet, thereby restraining the conduit from rotating. Both the shims and pins are shown in Fig. 1(c). The 2nd collet was translated down the conduit length in synchronization with the lathe turns. The ratio of lathe rotation to collet translation was calculated a priori to again target a ∼25 cm twist pitch.

It is worth noting that the pins of the translating collet benefited from the use of *full-length* pins for this configuration, seen at the right of Fig. 2. For the collet in the lathe, the pins only needed to be as long as the collet pieces, as it was going to be stationary during twisting.

E. Conduit Bending

After twisting, the conduits were bent at room temperature using a Baleigh (Model R-M7) 3-point manual rolling radius

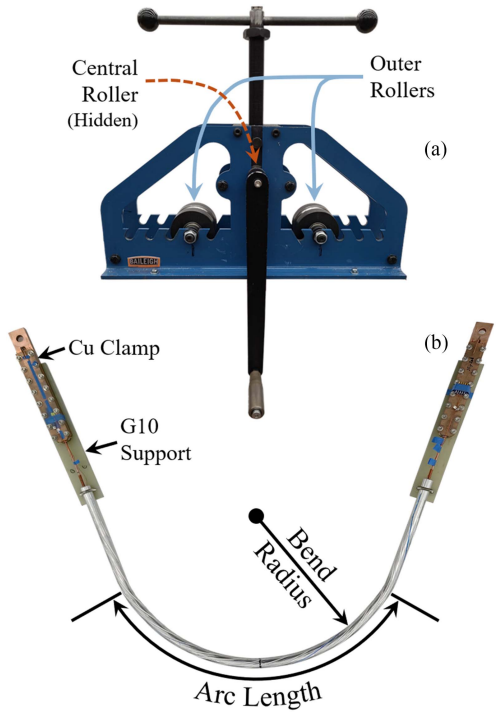

Fig. 3. (a) The baleigh R-M7 3-point bender used in this study. (b) The entire test assembly of a twisted & bent conduit and Cu clamps at the ends.

bender. (Fig. 3(a)) With the two outside (lower) rollers spaced ∼20 cm apart, the twisted conduit was centrally placed, and the top central roller was lowered until in contact with the conduit. For each pass, the top central roller was lowered 1 mm.

Each pass was taken to ∼2–3 mm less in conduit length than the previous pass. This was due a developing kink in the conduit at the endpoint of each pass length, when this was *not* done. However, a subtle kink could not be fully avoided with the bending method described here.

Also, the two arms of the bent conduit could get more and more out of plane with each pass, presumably an effect of the conduit's twist. This was ameliorated by simply manually pushing on them while rolling. A representative image of a twisted & bent conduit with CORC® and Cu clamps is shown in Fig. 3(b).

Table I shows the final measured twist pitches, bend radii, and arc-lengths for the CICCs used in this study. Electrical continuity checks with a handheld digital multimeter confirmed there were no electrical shorts between CORC® and conduit (at least, >60 MΩ), indicating intact insulation.

F. I_c Measurements

I_c was measured in liquid nitrogen (LN2) and self-field. The current was increased in a stepwise fashion until 30–70 μV was attained, with the voltage being measured by Keithley 2182A nanovoltmeters. The step size was smaller at low current to better determine the resistive baseline, then increased in the 'middle' current region, and then lowered again near the superconducting transition. The current was held for 1–2 seconds at each step before a voltage measurement was taken to minimize inductive pick-up.

TABLE I
DEFORMATION CHARACTERISTICS OF MEASURED CICCS

Cable ID	Condition	Twist Pitch	Bend Radius	Arc Length	Plot Category
Cable 1	Straight	---	---	---	Straight
	Twisted	24 cm (Stationary Twist)	---	---	Twisted
	Twist + Bend		53 cm	60 cm	Low Bend
	Twist + Bend		30 cm		Med Bend
	Twist + Bend		22 cm		Hi Bend
Cable 2	Straight	---	---	---	Straight
	Twisted	26 cm (Stationary Twist)	---	---	Twisted
	Twist + Bend		44 cm	65 cm	Low Bend
	Twist + Bend		34 cm		Med Bend
	Twist + Bend		24 cm		Hi Bend
Cable 3	Straight	---	---	---	Straight
	Twisted	33 cm (Translating Twist)	---	---	Twisted
	Twist + Bend		51 cm	67 cm	Low Bend
	Twist + Bend		33 cm		Med Bend
	Twist + Bend		25 cm		Hi Bend

The voltage was measured between the innermost, central-most and outermost voltage tap pairs, but only those at the innermost position are presented here. The innermost taps had the least resistive (but non-zero) baseline. I_c was defined as the current where 20 μV was attained, after subtraction of the resistive baseline. 20 μV equates to an electric field criterion of ∼0.15 μV/cm.

There were 3 consecutive I_c runs per sample per deformation state. The LN2 bath temperature was measured with a Cernox sensor for all runs, except for the first 2 deformation states of Wire #1. No temperature-based I_c corrections were made, as the measured temperatures were all very close, allowing for relative I_c comparisons.

n-value was determined using the data points that were both (1) nearest to the 20 μV criterion and (2) linear in log-log space. The relatively low I_c criterion was to protect the CORC® wire, as there was no automatic quench protection for this test set-up.

III. RESULTS AND DISCUSSION

Table II shows the I_c and *n*-values for the 3 wires at all deformation states. The reported values are the average of the 3 I_c runs, except for the "Medium Bend' of Wire #1, for which only one run could be analyzed due to excessive voltage noise.

When plotted as shown in Fig. 4, normalized I_c can be seen to generally decrease with increasing deformation, which is not surprising. However, it appears that the normalized I_c, for Wires #2 & #3 is approaching a plateau at ∼11% degradation, and similarly for Wire #1 but at ∼3% degradation. All three wires show ∼5% degradation due solely to bending (i.e., from the twisted-but-straight state to the smallest bend radius). Despite this plateau, it is expected that the I_c will continue to degrade with increasing bending deformation (i.e., smaller bend radii).

Wire #1 was the only wire for which the I_c *increased* after twisting. This was interesting considering Wire #2 came from

TABLE II
MEASURED I_C AND N-VALUES

Wire ID	Plot Category	Avg I_c (A)	σ I_c (A)	Normalized I_c	Avg n-val	σ n-val	Temp (K)
Wire 1	Straight	1051	9.51	1.000	12.5	0.29	NM
	Twisted	1074	3.11	1.022	11.0	0.45	NM
	Low Bend	1032	4.03	0.982	9.9	1.56	77.27
	Med Bend	1024*	---	0.974	9.9	---	77.28
	Hi Bend	1014	0.73	0.965	10.0	0.59	77.36
Wire 2	Straight	1142	7.75	1.000	12.0	2.38	77.24
	Twisted	1071	3.66	0.939	9.0	0.55	77.25
	Low Bend	1054	3.88	0.923	8.5	0.24	77.20
	Med Bend	1017	11.98	0.891	7.9	0.40	77.30
	Hi Bend	1021	1.80	0.895	7.8	0.06	77.21
Wire 3	Straight	1861	9.55	1.000	14.8	1.22	77.25
	Twisted	1759	7.74	0.945	10.2	3.71	77.27
	Low Bend	1691	5.12	0.909	6.9	0.71	77.25
	Med Bend	1662	2.25	0.893	7.2	0.74	77.24
	Hi Bend	1651	7.62	0.887	6.8	0.40	77.22

* Single value measurement
NM = Not Measured

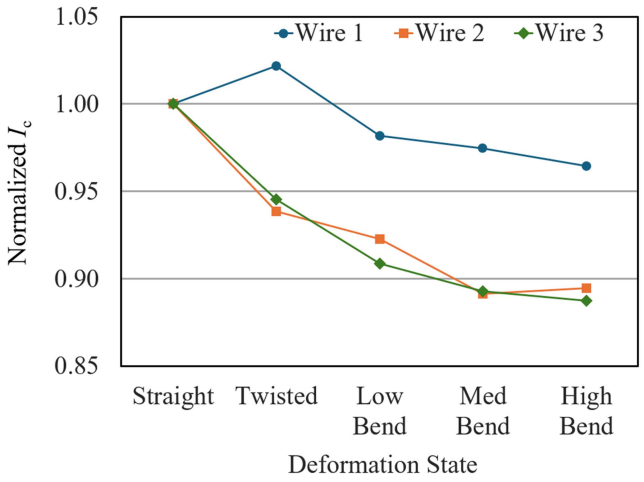

Fig. 4. Normalized I_c vs deformation state. All wires showed a similar relative I_c decline with bending.

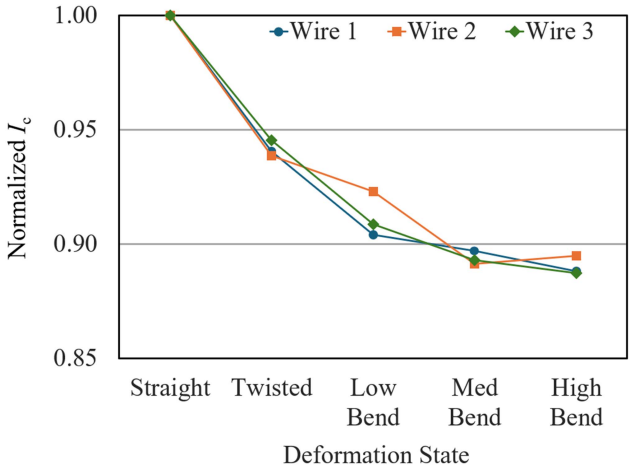

Fig. 5. Normalized I_c vs deformation state, after Wire #1's Straight I_c was replaced with that of Wire #2. All curves are well aligned, including after only twisting, unlike Fig. 4.

the same source material, but Wire #2 behaved more like one might expect, with an I_c degradation after twisting and beyond. LN2 bath temperatures were not measured during the straight and twisted-only runs of Wire #1, but it should not have been a significant influencer. [18] Regardless, this measurement seems erroneous for an unknown reason(s).

Since (1) the I_c values of Wire #1 are very close to those of Wire #2 at all other deformation states, and (2) Wire #1 & #2 are from the same source material, a quick check was made by artificially using the Wire #2 straight I_c value for that of Wire #1. The resultant normalized I_c curves are shown in Fig. 5. Interestingly, all curves now follow the same overall curve, with all wires showing ~11% degradation.

Fig. 5 is compelling in that it indicates that not only are the deformation-related I_c characteristics repeatable within a wire (Wires #1 & #2), but they may also be reproduceable (in normalized space) for other similar CORC® wires that use tape from other manufacturers (Wire #3).

In attempting to twist a 2.4 m (8 ft) long conduit by simply holding each end, it was noticed that the twist pitch was not uniform along the length and the conduit developed a subtle helical shape. The non-uniform twist pitch and helicity were made negligible by shortening the conduit to 1.2 m, and thus allowed the manufacture of samples #1 & #2 in this study. However, real world conductors will need to be longer than this, which prompted the new 'translating collet' technique.

The translating collet method could possibly be scaled up to meters-long lengths of continuous, uniform conduit twisting with CORC® wires inside. The theory of operation is that, as the collet translates down the conduit, the fresh non-twisted conduit that emerges has a small amount less coldwork than the twisted conduit that preceded it. Therefore, the twisting occurs preferentially at this location.

Wire #3 was successfully twisted this new way. In Fig. 5, the normalized I_c trend of Wire #3 matched that of the wires twisted in the more standard way, despite this manufacturing difference (and despite the ReBCO tape manufacturer difference).

It was also observed that, in the translating collet technique, the CORC® wire wraps around the central axis of the conduit without in a planetary-like motion, minimizing or eliminating torsional stress on the CORC® wire.

n-values show a decrease with increasing deformation, indicating increasing heterogeneity in individual tape I_c values within the CORC®. However, n-values from these low electric fields might not be the most illustrative or definitive, as there is still current sharing occurring between tapes when the transition is just beginning [19]. Regardless, they are included for completeness.

As next steps, vacuum impregnation studies are planned, whereby the void between conductor and conduit are filled to

help address Lorentz forces and potential conductor movement. In addition, quench experiments are also planned.

IV. Conclusion

A CORC® conductor has been twisted and bent inside a 6-around-1 aluminum conduit, in an effort to simulate the amount of deformation in a real-world machine. It was found that twisting to a ∼25 cm pitch caused as much as 6% degradation, and subsequent bending to a radius of ∼25 cm caused ∼5% I_c additional degradation.

References

[1] A. Vaskuri, B. Curé, A. Dudarev, and M. Mentink, "Aluminium-stabilized high temperature superconducting cable for particle detector magnets," *IEEE Trans. Appl. Supercond.*, vol. 30, no. 5, Aug. 2023, Art. no. 4500506, doi: 10.1109/TASC.2023.3262770.

[2] A. Ballarino, "Challenge of HTS for future accelerator magnets," *Superconducting Detector Magnet Workshop,* Geneva, Switzerland, Sep. 14, 2022.

[3] L. Muzzi, G. De Marzi, A. Di Zenobio, and A. della Corte, "Cable-in-conduit conductors: Lessons from the recent past for future developments with low and high temperature superconductors," *Supercond. Sci. Technol.*, vol. 28, no. 5, Mar. 2015, Art. no. 053001, doi: 10.1088/0953-2048/28/5/053001.

[4] N. Mitchell, "Cable-in-conduit conductor (CICC) experience in ITER," *Superconducting Detector Magnet Workshop*, Geneva, Switzerland, Sep. 14, 2022.

[5] J. Weiss, T. Mulder, H. ten Kate, and D. van der Laan, "Introduction of CORC wires: Highly flexible, round high-temperature superconducting wires for magnet and power transmission applications," *Supercond. Sci. Technol.*, vol. 30, no. 1, Nov. 2016, Art. no. 014002, doi: 10.1088/0953-2048/30/1/014002.

[6] V. Anvar et al., "Bending of CORC cables and wires: Finite element parametric study and experimental validation," *Supercond. Sci. Technol.*, vol. 31, no. 11, Oct. 2018, Art. no. 115006, doi: 10.1088/1361-6668/aadcb9.

[7] G. Xiao, C. Zhou, J. Qin, H. Jin, P. Xu, and H. Liu, "Experimental study on the critical current of CORC cable under cyclic bending-straightening," *IEEE Trans. Appl. Supercond.*, vol. 31, no. 8, Nov. 2021, Art. no. 4803904, doi: 10.1109/TASC.2021.3101753.

[8] J. Zhang, J. Zheng, Y. Song, F. Jiang, and X. Wang, "Study of the influence of helical bending strain and perpendicular self-field on critical current degradation for multilayer YBCO tapes," *IEEE Trans. Appl. Supercond.*, vol. 26, no. 8, Dec. 2016, Art. no. 8402806, doi: 10.1109/TASC.2016.2607157.

[9] T. Mulder, J. Weiss, D. van der Laan, A. Dudarev, and H. ten Kate, "Recent progress in the development of CORC cable-in-conduit conductors," *IEEE Trans. Appl. Supercond.*, vol. 30, no. 4, Jun. 2020, Art. no. 4800605, doi: 10.1109/TASC.2020.2968251.

[10] Y. Wu et al., "Mechanical analysis of CORC CICC for future fusion CS magnet," *IEEE Trans. Appl. Supercond.*, vol. 34, no. 5, Aug. 2024, Art. no. 4802905, doi: 10.1109/TASC.2024.3362734.

[11] Y. Narushima et al., "Test of 10 kA-class HTS WISE conductor in high magnetic field facility," *Plasma Fusion Res.*, vol. 17, Apr. 2022, Art. no. 2405006, doi: 10.1585/pfr.17.2405006.

[12] G. Celentano et al., "Design of an industrially feasible twisted-stack HTS cable-in-conduit conductor for fusion application," *IEEE Trans. Appl. Supercond.*, vol. 24, no. 3, Jun. 2014, Art. no. 4601805, doi: 10.1109/TASC.2013.2287910.

[13] M. Takayasu, L. Chiesa, N. Allen, and J. Minervini, "Present status and recent developments of the twisted stacked-tape cable conductor," *IEEE Trans. Appl. Supercond.*, vol. 26, no. 2, Mar. 2016, Art. no. 6400210, doi: 10.1109/TASC.2016.2521827.

[14] N. Castaneda et al., "A 6-around-1 cable using high-temperature superconducting STAR wires for magnet applications," *Supercond. Sci. Technol.*, vol. 37, no. 3, Mar. 2024, Art. no. 035009, doi: 10.1088/1361-6668/ad20fb.

[15] D. van der Laan, "Superconducting cable connections and methods," U.S. Patent 9755329 B2, Sep. 05, 2017.

[16] D. van der Laan, "Superconducting cable connections and methods," EP Patent 3008777 A1, Nov. 06, 2019.

[17] N. Mitchell et al., "Superconductors for fusion: A roadmap," *Supercond. Sci. Technol.*, vol. 34, no. 10, Sep. 2021, Art. no. 103001, doi: 10.1088/1361-6668/ac0992.

[18] D. van der Laan, J. Weiss, C. Kim, L. Graber, and S. Pamidi, "Development of CORC cables for helium gas cooled power transmission and fault current limiting applications," *Supercond. Sci. Technol.*, vol. 31, no. 5, Jul. 2018, Art. no. 085011, doi: 10.1088/1361-6668/aacf6b.

[19] V. Phifer, "Experimental investigations of tape-to-tape contact resistance and its impact on current distribution around local I_c degradations in CORC cables," Ph.D. dissertation, Dept. Mech. Eng., Florida State Univ., Tallahassee, FL, USA, 2023.